ORGANIC LETTERS

2013
Vol. 15, No. 19
5092–5095

Cage Size Effects on the Rotation of Molecular Gyrotops with 1,4-Naphthalenediyl Rotor in Solution

Wataru Setaka,*,† Akiko Koyama,‡ and Kentaro Yamaguchi‡

Division of Applied Chemistry, Faculty of Urban Environmental Sciences, Tokyo Metropolitan University, 1-1 Minami-Osawa, Hachioji, Tokyo 192-0397, Japan, and Faculty of Pharmaceutical Sciences at Kagawa Campus, Tokushima Bunri University, 1314-1 Shido, Sanuki, Kagawa 769-2193, Japan

wsetaka@tmu.ac.jp

Received August 26, 2013

ABSTRACT

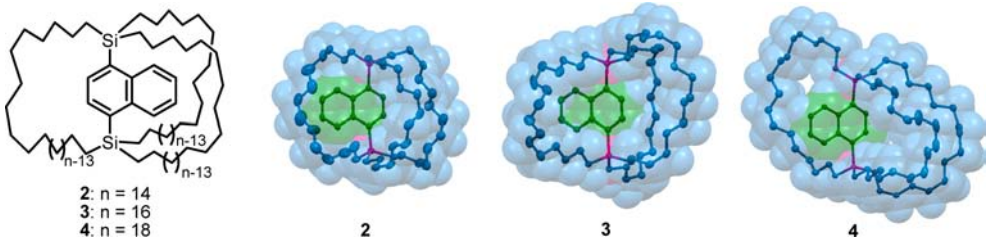

1,4-Naphthalenediyl-bridged macrocages (2, 3, and 4) were synthesized as novel molecular gyrotops. Compound 2 (C14 chains) does not show rotation of the naphthalene ring about an axis in solution. The 1,4-naphthalenediyl moieties of compounds 3 (C16 chains) and 4 (C18 chains) show restricted and rapid rotation inside the cage in solution, respectively. Therefore, steric protective effects on the rotation of the rotor in molecular gyrotops can be controlled by changing the size of the cage.

Much attention is currently focused on the chemistry of molecular machines exhibiting mechanical motions of the molecular components.[1] The analysis of their structure and dynamics is important because molecular motion is likely to affect physical and chemical properties. Macrocage molecules with a bridged rotor are of interest because they are expected to act as molecular gyroscopes, which is a class of molecular machines.[2−5]

We recently reported the synthesis and properties of crystalline molecular gyrotops that have a phenylene rotor encased by three long alkyl spokes.[4,5] In particular, molecular gyrotop **1** (Figure 1) allowed thermal modulation of the birefringence of a single crystal, reported as the first application of the variation of optical properties due

† Tokyo Metropolitan University.
‡ Tokushima Bunri University.

(1) (a) Vogelsberg, C. S.; Garcia-Garibay, M. A. *Chem. Soc. Rev.* **2012**, *41*, 1892. (b) Karim, A. R.; Linden, A.; Baldridge, K. K.; Siegel, J. S. *Chem. Sci.* **2010**, *1*, 102. (c) Blanzani, V.; Credi, A.; Venturi, M. *Molecular Devices and Machines*, 2nd ed.; Wiley-VCH: Weinheim, Germany, 2008. (d) Leigh, D. A.; Zerbetto, F.; Kay, E. R. *Angew. Chem., Int. Ed.* **2007**, *46*, 72. (e) Browne, W. R.; Feringa, B. L. *Nat. Nanotechnol.* **2006**, *1*, 25. (f) Kelly, T. R. *Molecular Machines. Topics in Current Chemistry*; Springer: Heidelberg, 2005; Vol. 262. (g) Kottas, G. S.; Clarke, L. I.; Horinek, D.; Michl, J. *Chem. Rev.* **2005**, *105*, 1281. (h) Garcia-Garibay, M. A. *Proc. Natl. Acad. Sci. U.S.A.* **2005**, *102*, 10771. (i) Blanzani, V.; Credi, A.; Raymo, R.; Stoddart, J. F. *Angew. Chem., Int. Ed.* **2000**, *39*, 3348.

(2) (a) Dominguez, Z.; Dang, H.; Strouse, M. J.; Garcia-Garibay, M. A. *J. Am. Chem. Soc.* **2002**, *124*, 2398. (b) Godinez, C. E.; Zepeda, G.; Garcia-Garibay, M. A. *J. Am. Chem. Soc.* **2002**, *124*, 4701. (c) Dominguez, Z.; Dang, H.; Strouse, J. M.; Garcia-Garibay, M. A. *J. Am. Chem. Soc.* **2002**, *124*, 7719. (d) Dominguez, Z.; Khuong, T. A. V.; Sanrame, C. N.; Dang, H.; Nuñez, J. E.; Garcia-Garibay, M. A. *J. Am. Chem. Soc.* **2003**, *125*, 8827. (e) Commins, P.; Nuñez, J. E.; Garcia-Garibay, M. A. *J. Org. Chem.* **2011**, *76*, 8355. (f) Nuñez, J. E.; Natarajan, A.; Khan, S. I.; Garcia-Garibay, M. A. *Org. Lett.* **2007**, *9*, 3559. (g) Commins, P.; Nuñez, J. E.; Garcia-Garibay, M. A. *J. Org. Chem.* **2011**, *76*, 8355. (h) Czajkowska-Szczykowska, D.; Rodríguez-Molina, B.; Magaña-Vergara, N. E.; Santillan, R.; Morzycki, J. W.; Garcia-Garibay, M. A. *J. Org. Chem.* **2012**, *77*, 9970. (i) Rodríguez-Molina, B.; Pérez-Estrada, S.; Garcia-Garibay, M. A. *J. Am. Chem. Soc.* **2013**, *135*, 10388.

(3) (a) Shima, T.; Hampel, F.; Gladysz, J. A. *Angew. Chem., Int. Ed.* **2004**, *43*, 5537. (b) Shima, T.; Bauer, E. B.; Hampel, F.; Gladysz, J. A. *Dalton Trans.* **2004**, 1012. (c) Nawara, A. J.; Shima, T.; Hampel, F.; Gladysz, J. A. *J. Am. Chem. Soc.* **2006**, *128*, 4962. (d) Wang, L.; Hampel, F.; Gladysz, J. A. *Angew. Chem., Int. Ed.* **2006**, *45*, 4372. (e) Wang, L.; Shima, T.; Hampel, F.; Gladysz, J. A. *Chem. Commun.* **2006**, 4075. (f) Hess, G. D.; Hampel, F.; Gladysz, J. A. *Organometallics* **2007**, *26*, 5129. (g) Skopek, K.; Gladysz, J. A. *J. Organomet. Chem.* **2008**, *693*, 857. (h) Skopek, K.; Barbasiewicz, M.; Hampel, F.; Gladysz, J. A. *Inorg. Chem.* **2008**, *47*, 3474.

10.1021/ol402464d
Published on Web 09/19/2013

to the dynamics of the phenylene rotor in a crystal.[5a] The derivatives of **1** showed remarkable expansion of the cage in the crystalline state due to the rapid rotation of the phenylene rotor, and an exceptionally high thermal expansion coefficient of the crystal was estimated, suggesting a new function for the dynamic states of the molecules.[5b]

In solution, however, these molecular gyrotops (i.e., **1** and its derivatives) show rapid rotation of the phenylene rotor because the ^{1}H NMR signals of three tetradecyl spokes of the compound are identical in $CDCl_3$. Controlling the rotation, such as its direction and energy barriers, may allow construction of novel functional materials based on the dynamic states or kinetics of the rotor. In this report, we designed and synthesized novel molecular gyrotops (**2**, **3**, and **4**; Figure 1) with a bulky 1,4-naphthalenediyl rotor and show the chain length dependence of the crystal structures and the energy barrier in the rotation of the rotor in solution.

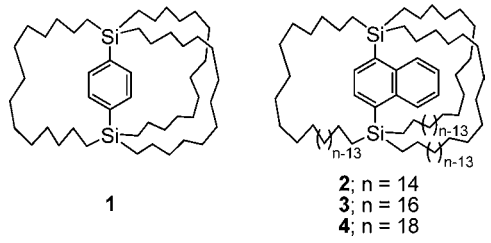

Figure 1. Structures of molecular gyrotops.

The synthesis of molecular gyrotops (**2**, **3**, and **4**) is shown in Scheme 1, which is almost identical to the previously reported synthesis of **1**.[5] The molecular gyrotops (**2**–**4**) were synthesized by ring-closing metathesis of *p*-bis(tri-ω-alkenyl)silylnaphthalenes (**5**–**7**) prepared by the reaction of dilithionaphthalenes with corresponding tri-ω-alkenylchlorosilanes and the hydrogenation by H_2 gas (3 atm) in the presence of Pd/C catalyst.[6]

Scheme 1. Synthesis of Molecular Gyrotops **2**–**4**

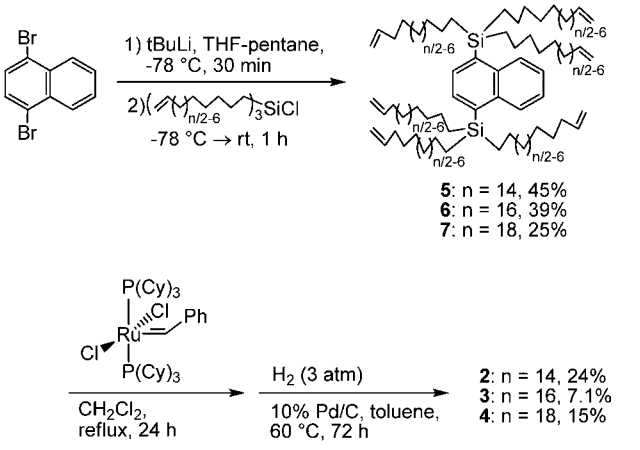

The desired cage-like isomers were isolated by preparative GPC of the reaction mixture, which also contained noncage isomers and polymeric byproducts. Compounds **2**, **3**, and **4** were identified by ^{1}H, ^{29}Si, and ^{13}C NMR spectroscopy.[6]

Molecular gyrotops **2**, **3**, and **4** were crystallized to give single crystals suitable for X-ray diffraction studies via recrystallization from a tetrahydrofuran/methanol mixture (4:1 v/v) solution. Figure 2 shows the molecular structures of molecular gyrotops **2**–**4** in a single crystal, determined by X-ray crystallography at 120 K.[7] In all compounds, three alkyl chains effectively surrounded the bis-silylnaphthalene moiety, and the molecules were packed in crystals and arranged according to their rotation axes. In addition, molecular gyrotops **3** and **4** exist as π-stacked aggregates of two molecules in a crystal, where the naphthalene rings are arranged face-to-face.[6] In particular, in the case of **3**, two kinds of aggregates were observed: one is a π-stacked aggregate (type A), and the other has two tetrahydrofurans between the naphthalene rings (type B). The distances between the two naphthalene rings in the π-stacked aggregates are 3.56 Å for **2** (type A) and 3.46 Å for **3**. These values are close to the distance between the layers in graphite (3.354 Å[8]), indicating that a remarkable π–π interaction exists in the aggregates. On the other hand, molecular gyrotops **2** with the shortest alkyl chains (C14) did not form a π-stacking structure inside the crystal. Because the naphthalene ring, which is fixed between tight exterior spokes, is sterically protected by the cage, the formation of the π-stacked aggregate is prevented in **2**.

The dependence of the steric effects on the chain length of molecular gyrotops with a 1,4-naphthalenediyl rotor are also observed in solution. Figure 3 shows the ^{13}C NMR spectra of the molecular gyrotops observed at 300 K in $CDCl_3$. The spectrum of **4** with the largest cage shows nine methylene signals. The cage of **4** possesses quasi-D_3

(4) (a) Marahatta, A. B.; Kanno, M.; Hoki, K.; Setaka, W.; Irle, S.; Kono, H. *J. Phys. Chem. C* **2012**, *116*, 24845. (b) Setaka, W.; Ohmizu, S.; Kira, M. *Chem. Lett.* **2010**, *39*, 468. (c) Setaka, W.; Ohmizu, S.; Kabuto, C.; Kira, M. *Chem. Lett.* **2007**, *36*, 1076.

(5) (a) Setaka, W.; Yamaguchi, K. *Proc. Natl. Acad. Sci. U.S.A.* **2012**, *109*, 9260. (b) Setaka, W.; Yamaguchi, K. *J. Am. Chem. Soc.* **2012**, *134*, 12458. (c) Setaka, W.; Yamaguchi, K. *J. Am. Chem. Soc.* **2013**, DOI: 10.1021/ja408405f.

(6) See Supporting Information for details.

(7) Diffraction data of **1** were collected on a Bruker APEX-II CCD system using graphite-monochromatized Mo Kα radiation (λ = 0.71069 Å). Crystal data for **2** (120 K): $C_{52}H_{90}Si_2$, M = 771.42, triclinic, $P\bar{1}$, a = 13.327(3) Å, b = 17.391(4) Å, c = 23.422(5) Å, α = 93.875(3)°, β = 102.751(2)°, γ = 110.568(2)°, V = 4894.2(18) Å^3, density (calculated) 1.047 Mg/m^3, Z = 4, 1048 parameters, 72 restraints. Final R indices $R1$ = 0.0781 [$I > 2\sigma(I)$], $wR2$ = 0.2273 for all data, 17014 unique reflections. Crystal data for **3** (120 K): $2(C_{58}H_{102}Si_2)\cdot 1.5(C_4H_8O)$, M = 1819.31, triclinic, $P\bar{1}$, a = 14.1947(12) Å, b = 15.1832(13) Å, c = 28.719(2) Å, α = 85.1370(10)°, β = 80.2820(10)°, γ = 75.0800(10)°, V = 5889.5(9) Å^3, density (calculated) 1.026 Mg/m^3, Z = 2, 1247 parameters, 54 restraints. Final R indices $R1$ = 0.0589 [$I > 2\sigma(I)$], $wR2$ = 0.1625 for all data, 22315 unique reflections. Crystal data for **4** (120 K): $C_{64}H_{114}Si_2$, M = 3063.4, triclinic, $P\bar{1}$, a = 14.5354(18) Å, b = 14.7161(18) Å, c = 16.738(2) Å, α = 66.601(2)°, β = 82.719(2)°, γ = 68.828(2)°, V = 3063.4(6) Å^3, density (calculated) 1.019 Mg/m^3, Z = 2, 614 parameters, 5 restraints. Final R indices $R1$ = 0.0589 [$I > 2\sigma(I)$], $wR2$ = 0.1511 for all data, 11731 unique reflections. Crystallographic data were deposited in the Cambridge Crystallographic Database Centre (CCDC-957186 for **2**, CCDC-957187 for **3**, CCDC-957188 for **4**).

(8) Franklin, R. E. *Acta Crystallogr.* **1951**, *4*, 253.

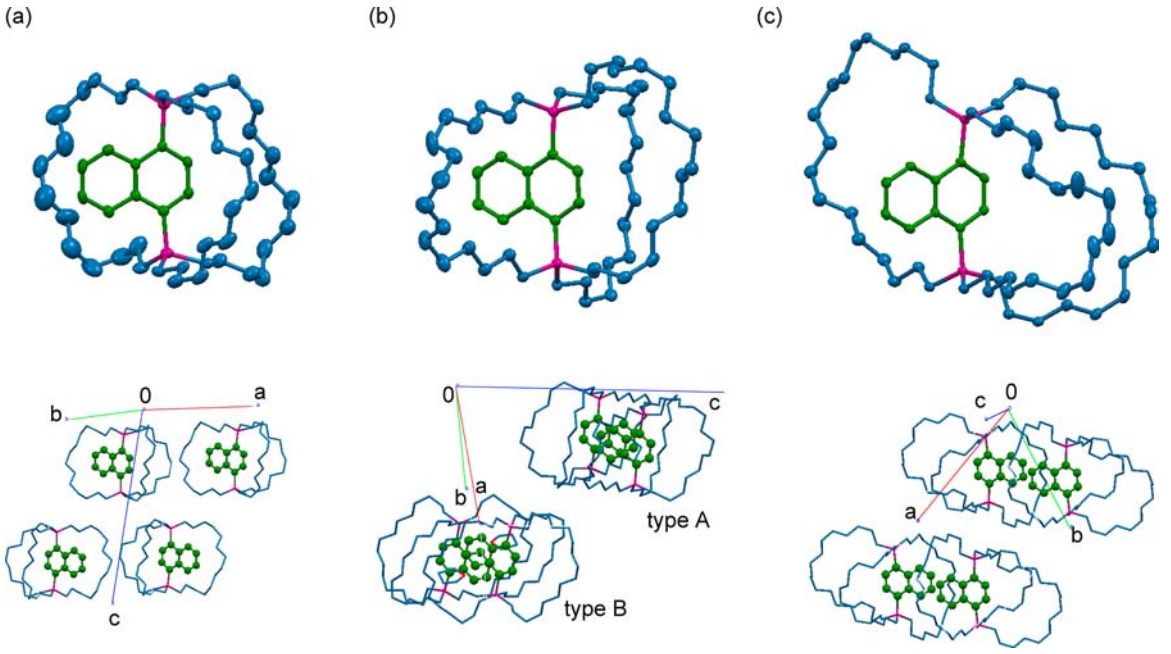

Figure 2. Molecular structures of compounds (a) **2**, (b) **3**, and (c) **4**. Top: equatorial view with 30% thermal probability ellipsoid. Bottom: packing diagram. Hydrogen atoms, THF molecules in the packing diagram of **2**, and disordered atoms on the side chains are omitted for clarity.

symmetry, indicating that three alkyl chains are identical in the time scale of the NMR measurement because the naphthalene ring rotates rapidly inside the cage. Therefore, the methylene groups adjacent to silicon atoms give identical chemical shifts at 13.8 ppm. On the other hand, the NMR spectrum of **2** shows 14 methylene signals, and half of them have two times higher intensities. Therefore, the cage of **2** possesses quasi-C_{2v} symmetry, indicating that two of the three alkyl chains are identical in the time scale of the NMR measurement because the rotation of the naphthalene ring is almost stopped inside the cage. Therefore, methylene signals adjacent to silicon atoms were divided by two signals at 13.1 and 15.2 ppm. In the case of the NMR spectrum of **3**, some methylene signals were observed as broad signals, indicating that rotation of the naphthalene ring in the cage is slower than the NMR time scale.

The temperature dependence of the ^{13}C NMR spectra of **3** in toluene-d_8 is shown in Figure 4. The spectra were obtained by using an inverse gated decoupling pulse sequence to suppress NOE effects. The spectrum at 220 K shows the two kinds of signals of methylenes adjacent to silicon atoms at 11.4 and 14.5 ppm. These signals become broader with increasing temperature and coalesce at around 290 K. The dynamic ^{13}C NMR behavior of **3** is explained by assuming an equilibrium between three equivalent conformations **3**, **3′**, and **3″** shown in Figure 5. The exchange rate constants (k_{ex}) were determined by line

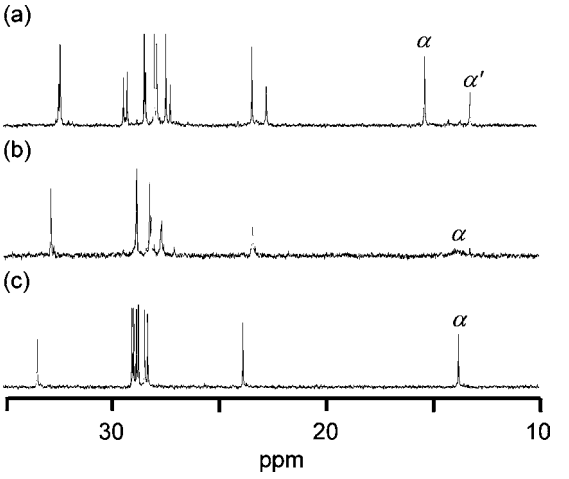

Figure 3. ^{13}C NMR spectra of compounds (a) **2**, (b) **3**, and (c) **4** in $CDCl_3$ at 300 K (methylene region). The symbols α and α′ indicate signals assignable to methylene carbons adjacent to silicon atoms.

shape analysis assuming a three-site exchange model, and the simulation was carried out at 320 K for three representative methylene signals labeled as α, β, and γ in Figure 4 (the assignments of these signals are shown in Figure 5).[9]

The Eyring parameters for the exchange determined from the linear plots of $\ln(k_{ex}/T)$ versus $1/T$ are $\Delta H^{\ddagger} = 9.42 \pm 0.08$ kcal mol^{-1} and $\Delta S^{\ddagger} = -12.0 \pm 0.3$ cal mol^{-1} K^{-1}

(9) gNMR software was used for the calculations (gNMR: v.4.1.0 for Windows, IvorySoft, 1999).

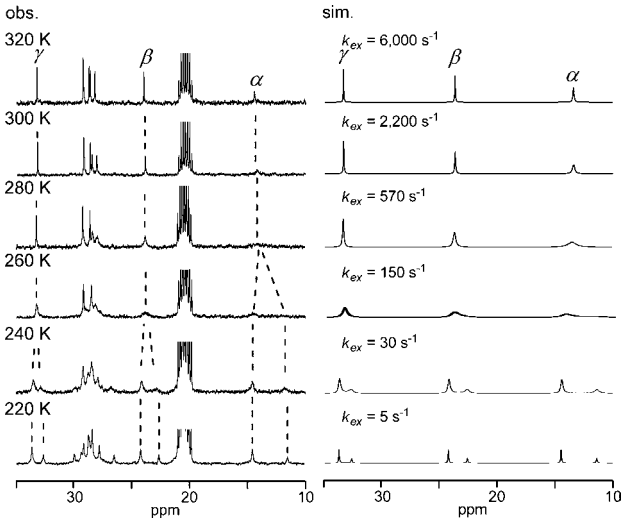

Figure 4. Temperature dependence of inverse gated decoupling ^{13}C NMR spectra of **3** in toluene-d_8 (methylene region). Left: observed spectra. Right: simulated spectra for the representative signals α, β, and γ with designated exchange rate constants (k_{ex}).

for **3**.[6] The large negative $\Delta S^{\ddagger}$ value for the rotation of the naphthalene ring inside the cage of **3** indicates a tight dynamic transition state. In addition, the ^{13}C NMR spectra of **2** and **4** in toluene-d_8 showed no temperature dependence in the temperature range from 220 to 340 K because the molecular motions of these compounds are outside the time scale of the NMR measurement.[6] Therefore, the activation enthalpies for the rotation of the naphthalene ring inside the cage are estimated to be above and below 10 kcal/mol for **2** and **4**, respectively.

In summary, 1,4-naphthalenediyl-bridged macrocages (**2**, **3**, and **4**) were synthesized as novel molecular gyrotops, and they showed chain length dependence of the crystal

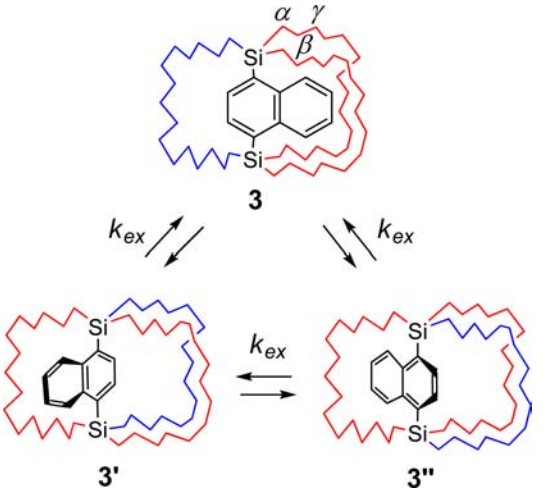

Figure 5. Schematic representation of naphthalene ring rotation about the axis in **3**.

structure and energy barrier for the rotation of the naphthalene ring in solution. Therefore, steric protective effects of the molecular gyrotops can be controlled by changing the size of the cage.

Acknowledgment. This work was supported by a JSPS Grant-in-Aid for Scientific Research (B) (No. 25288042).

Supporting Information Available. Details of the synthesis, X-ray crystallographic analysis, temperature-dependent ^{13}C NMR spectra, and crystallographic information for molecular gyrotops **2**, **3**, and **4**. This material is available free of charge via the Internet at http://pubs.acs.org.

The authors declare no competing financial interest.